Skin Research and Technology 2014; **20**: 445–452
Printed in Singapore · All rights reserved
doi: 10.1111/srt.12139

Skin Research and Technology

Investigation of the mechanical behaviour of the foot skin

C. G. Fontanella[1], E. L. Carniel[1,2], A. Forestiero[1,2] and A. N. Natali[1,2]

[1]Centre of Mechanics of Biological Materials, University of Padova, Padova, Italy and [2]Department of Industrial Engineering, University of Padova, Padova, Italy

Background/purpose: The aim of this work was to provide computational tools for the characterization of the actual mechanical behaviour of foot skin, accounting for results from experimental testing and histological investigation. Such results show the typical features of skin mechanics, such as anisotropic configuration, almost incompressible behaviour, material and geometrical non linearity. The anisotropic behaviour is mainly determined by the distribution of collagen fibres along specific directions, usually identified as cleavage lines.

Methods: To evaluate the biomechanical response of foot skin, a refined numerical model of the foot is developed. The overall mechanical behaviour of the skin is interpreted by a fibre-reinforced hyperelastic constitutive model and the orientation of the cleavage lines is implemented by a specific procedure. Numerical analyses that interpret typical loading conditions of the foot are performed. The influence of fibres orientation and distribution on skin mechanics is outlined also by a comparison with results using an isotropic scheme.

Results: A specific constitutive formulation is provided to characterize the mechanical behaviour of foot skin. The formulation is applied within a numerical model of the foot to investigate the skin functionality during typical foot movements. Numerical analyses developed accounting for the actual anisotropic configuration of the skin show lower maximum principal stress fields than results from isotropic analyses.

Conclusion: The developed computational models provide reliable tools for the investigation of foot tissues functionality. Furthermore, the comparison between numerical results from anisotropic and isotropic models shows the optimal configuration of foot skin.

Key words: foot skin biomechanics – cleavage lines – constitutive formulation – hyperelasticity – finite element model

Accepted for publication 5 January 2014

THE SKIN is a living complex material and its major functions are the regulation of body temperature, protection, excretion and absorption. With regard to the mechanical and structural configuration, the skin binds up the underlying soft tissues. The skin is mainly composed of two layers, epidermis and dermis, which provide different mechanical contributions. The dermis is composed of cells and fibrous proteins such as collagen and elastin. These fibrous proteins define a dense meshwork of fibres and fibre bundles embedded within a ground substance. In the context of a fibre-reinforced composite material, fibrous proteins, with particular regard to collagen, are the reinforcing fibres, while the ground substance is the isotropic matrix (1).

The specific orientation of the collagen fibres determines the characteristic anisotropic response of the skin (2). The natural orientation of collagen fibres was noticed by Langer (3, 4), who observed that circular holes punched out in a cadaver skin became enlarged and elliptical due to predominant pre-stress along and across the major axes of the ellipse. While the Langer lines are the best known skin tension lines, other lines have been proposed as the Cox lines (5), the Bulacio's lines (6) and the relaxed skin tension lines (7). The existence of a grid of 'lines of non-extension' covering the human body surface was suggested by Iberall (8), who collected skin deformation data with a system of four infrared cameras that calculated the spatial position of reflective markers placed on the skin.

In general, all the distributions reported in the literature show that collagen fibres orientation depends on the specific location within the body, according to the motion of the local body joints or structures (9). With regard to the skin of the foot, different orientations of collagen fibres have been evaluated within the different regions of the foot. As a matter of example, studies report that the cleavage lines have a predominant organization in concentric circles around the basis of the heel, along mediolateral direction in the sole of the foot and along the anterior–posterior direction in the dorsal region (10).

A numerical modelling approach based on the finite element method is a robust tool to investigate foot skin biomechanics. Several numerical models of the human foot have been previously developed accounting for different assumptions, with particular regard to the morphological configuration, the constitutive formulations and the loading/boundary conditions (11–15). Different constitutive models have been assumed to interpret the mechanical behaviour of the skin. Gu et al. (16) studied the mechanical response of the hindfoot during the heel strike by a combined experimental and numerical approach. An isotropic Ogden hyperelastic formulation was applied to characterize the heel skin. Sopher et al. (17) developed an anatomically realistic three-dimensional finite element model of the heel region to study the risk of heel ulcers in bedridden patients. The mechanical behaviour of the heel skin was defined by an isotropic Ogden model.

The here proposed work reports a procedure to investigate the mechanics of foot skin with particular regard to the distribution of collagen fibres. The influence of the anisotropic configuration of the skin on the overall mechanical behaviour of the foot structures is investigated by a computational approach. At this purpose, a numerical model of a human foot is developed from CT and MRI images accounting for bones, soft connective tissues and skin. On the basis of histological data reported in literature, the distribution of collagen fibres is implemented within the numerical model by a specific procedure. An anisotropic fibre-reinforced hyperelastic formulation is developed to characterize the actual mechanical behaviour of the skin. To highlight the contribution of fibres on the mechanical response of the foot skin and its optimal configuration, the numerical results are compared with further results from numerical analysis performed assuming an isotropic hyperelastic formulation. In detail, the numerical analyses are developed accounting for typical foot movements, as dorsiflexion/plantarflexion, abduction/adduction and inversion/eversion.

Materials and methods

Histology and morphometry of the skin

Notes about the morphometry and the histology of the foot skin are reported to address the relationship between the structural configuration and the mechanical behaviour. The skin of the foot shows differences among the plantar and the dorsal regions. In the plantar foot, the skin is thickest in weight-bearing areas, as the heel and the metatarsal heads. In the dorsal foot, the skin is thin and makes the structures of the dorsal foot easily palpable. With regard to the histological configuration, the skin is a complex and multi-layered structure, composed of two layers, as the epidermis and the dermis, which are made of different tissues and have different functions. The thickness of the epidermis ranges between 0.14 and 0.8 mm, while the thickness of the dermis ranges between 0.9 and 1.3 mm (18, 19). The epidermis is made of stratified squamous epithelium, composed of stratum corneum, stratum lucidum, stratum granulosum, stratum spinosum and stratum basale. The skin of the sole has a thicker stratum corneum, a more marked stratum granulosum and a thicker stratum spinosum than the other regions of the foot (20). The dermis lies below the epidermis and is composed of cells and fibrous proteins, as collagen and elastin, embedded within a ground substance. The dermis is divided into two regions, papillary dermis and reticular dermis. The papillary layer is the superficial layer of the dermis, made up of loose areolar connective tissue with mainly elastic fibres. The reticular layer is more dense and thick and is mainly composed of collagen fibres and adipose tissue. Results from histological investigations show the peculiar distribution of collagen fibres along specific directions, aiming to the optimal mechanical functionality of the foot joints and structures (3–5, 7, 9).

Numerical model of the foot

A virtual solid model of the foot is developed accounting for bony segments, including the distal segments of tibia and fibula, cartilages, ligaments, adipose tissues, muscular tissues and skin (Fig. 1a). The models of bones are developed starting from CT images, while models of soft tissues are performed by the analysis of MRI data. The numerical model of the foot

(Fig. 1b, c) is obtained through the finite element discretization of the virtual solid model by the software MSC-Patran 2007 (MSC.Software Corporation, Santa Ana, CA, USA), adopting four node tetrahedral elements.

The mechanical behaviour of bone tissues is evaluated assuming an orthotropic linear elastic constitutive model (21); the ligaments mechanical response is defined by a fibre-reinforced visco-hyperelastic constitutive formulation (22); the adipose tissues mechanics is specified by a visco-hyperelastic model (23); and finally a hyperelastic Yeoh formulation is assumed for cartilaginous elements (24). The other soft tissue regions around the bony segments are considered to be homogeneous and the mechanical response is defined by an almost incompressible hyperelastic model (25). Particular attention is paid to the evaluation of the mechanical behaviour of skin tissue, as described in the following paragraph.

Fibre-reinforced constitutive formulation of skin tissue

Results from experimental tests and histological data (2, 26–28) show the typical features of skin mechanics, such as anisotropic configuration, almost incompressible behaviour, material and geometrical non linearity. The anisotropic behaviour of the skin is mainly determined by the distribution of collagen fibres (3, 4, 10, 29, 30).

The investigation of histological data (10) (Fig. 2a) makes it possible to identify the preferential orientation and distribution of collagen fibres, as the skin cleavage lines. In the dorsal region of the foot, the cleavage lines are oriented in the anterior–posterior direction, while near the toes, they are directed in the medial and lateral directions. In the lateral and medial foot, the cleavage lines are oriented to climb down the leg, wrapped around the ankle (Fig. 2b, c). As reported in Fig. 2d, within the sole of the foot, the cleavage lines have mediolateral direction while they have a predominant organization in concentric circles around the heel and the first metatarsal head.

Once the cleavage lines have been identified, a procedure for the implementation of the collagen fibres distribution within the numerical model of the foot skin must be provided. In detail, given the spatial coordinates of the generic Gauss point within the numerical model of the skin, the procedure has to provide the local collagen fibres unit vector. To this end, cleavage lines are interpolated by specific freeform poly-lines and a distribution of fibres vectors is provided by evaluating the poly-lines tangent vectors at different points, with an average distance of 5.0 mm from each other. With regard to the generic Gauss point, the fibres local direction is identified by averaging the tangent vectors at the three closest points of the previously defined set. Figure 3 reports the provided distribution of fibres directions within the numerical model of the skin.

Once the distribution of collagen fibres have been defined, the actual mechanical response of the skin is specified by a fibre-reinforced hyperelastic model (31). The model accounts for different contributions from the isotropic ground matrix (W_m) and the collagen fibres (W_f). The following general formulation of the strain energy is assumed:

$$W\left(\tilde{I}_1, I_3, I_4\right) = W_m\left(\tilde{I}_1, I_3\right) + W_f(I_4) \qquad (1)$$

Accounting for the almost incompressible behaviour of the tissue, the hyperelastic potential W_m can be split into volumetric U_m and iso-volumetric $\tilde{W}_m$ terms (23):

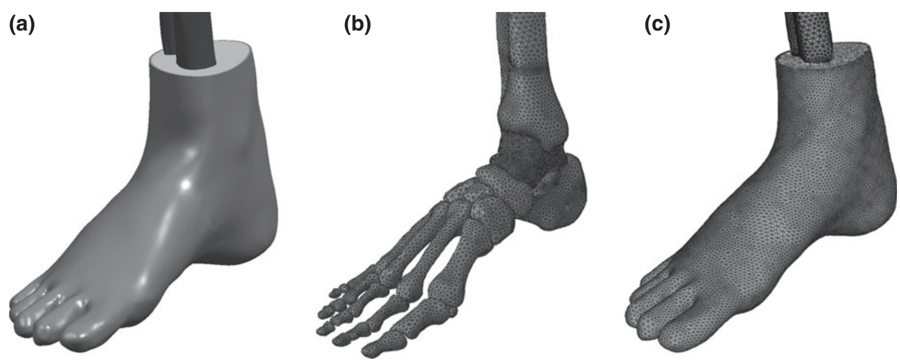

Fig. 1. Solid (a) and numerical (b and c) model of the foot.

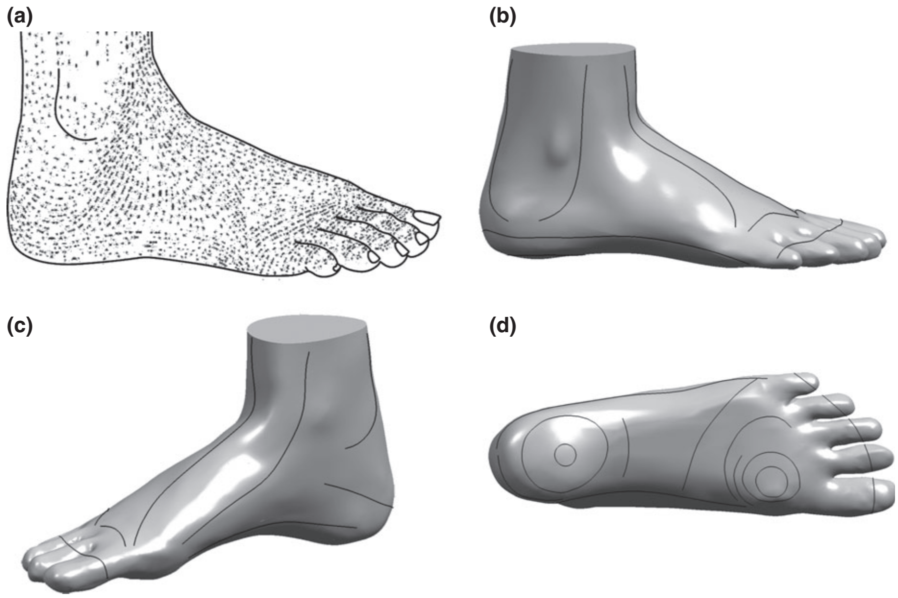

Fig. 2. Cleavage lines in the lateral view from histological data (a). Distribution of the some of the cleavage lines within the skin model: lateral (b), medial (c) and plantar (d) view.

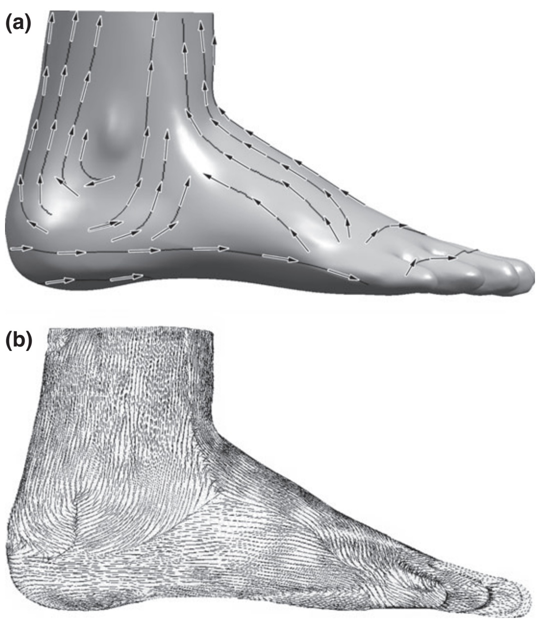

Fig. 3. Definition of the distribution of cleavage lines in the lateral region of the foot skin in the solid (a) and numerical (b) model.

$$W_{\mathrm{m}}(I_3, \tilde{I}_1) = U_{\mathrm{m}}(I_3) + \tilde{W}_{\mathrm{m}}(\tilde{I}_1) \qquad (2)$$

$$U_{\mathrm{m}}(I_3) = \frac{K_{\mathrm{v}}}{2 + r(r+1)}\left[\left(I_2^{1/2} - 1\right)^2 + I_3^{-r/2} + rI_3^{r1/2} - (r+1)\right] \qquad (3)$$

$$\tilde{W}_{\mathrm{m}}(\tilde{I}_1) = \frac{C_1}{\alpha}\left\{\exp\left[\alpha(\tilde{I}_1 - 3)\right] - 1\right\} \qquad (4)$$

where I_3 is the third invariant of the right Cauchy-Green strain tensor $\mathbf{C}$, as $I_3 = \det(\mathbf{C})$, $\tilde{I}_1$ is the first invariant of the iso-volumetric part of the right Cauchy-Green strain tensor, as $\tilde{I}_1 = \mathrm{tr}(\tilde{\mathbf{C}})$ and $\tilde{\mathbf{C}} = J^{-2/3}\mathbf{C}$. The constitutive parameters K_{v} and C_1 specify the initial volumetric and shear stiffness, respectively, while parameters r and α characterize the non-linear mechanical response because of the typical stiffening phenomena of soft biological tissues.

With regard to the fibres contribution W_{f}, I_4 is a structural invariant related to tissue stretch along the fibres direction. In the unstrained configuration, fibres are characterized by a wavy conformation. When tensile load is applied, fibres uncrimp and then get stretched. This mechanism determines a strongly non-linear mechanical response because of the gradual increase in the tissue stiffness along the fibres direction. A specific exponential formulation is provided:

$$W_{\mathrm{f}}(I_4) = \frac{C_4}{(\alpha_4)^2}\left\{\exp[\alpha_4(I_4 - 1)] - \alpha_4(I_4 - 1) - 1\right\} \qquad (5)$$

where C_4 defines the fibres initial stiffness, as $E_{\mathrm{f}} = 4C_4$, while α_4 depends on the initial wavy conformation of fibres (31). The anisotropic constitutive parameters are identified by analysing experimental data from compression tests developed along the skin thickness (32) and tensile tests developed along and normally to the principal axis of the skin (26). Analytical models are developed to interpret the experimental situations, accounting for the constitutive formulation and the specific boundary conditions. The discrepancy between model results and experimental data is evaluated by a cost function, whose minimization is performed by a stochastic-deterministic procedure (33) and entails the identification of the optimal set of constitutive parameters (34–36), which are reported in Table 1.

Numerical analysis of skin functionality

The numerical model is adopted to investigate the skin mechanical response accounting for several loading conditions, which stand for the typical movements of the ankle complex. The specific coordinate system adopted at this purpose (37) is represented in Fig. 4. In detail, the *X*-axis is defined as the line that joins the medial and the lateral malleulus. The perpendicular to the plane containing the lateral malleolus, the medial malleolus and the centroid of the tibial cross-section is the *Z*-axis. The *Y*-axis is consequently defined as the perpendicular to the plane spanned by *X*-axis and the *Z*-axis. The origin is located at the mid-point between the medial and the lateral malleulus. In detail, the dorsiflexion/plantarflexion, the inversion/eversion and the abduction/adduction movements are defined fixing the calcaneus and imposing a rotation of the tibia and the fibula around the *X*-axis, the *Z*-axis and the *Y*-axis respectively.

The evaluation of fibres contribution to foot skin functionality is performed by the investigation of skin mechanics accounting for both anisotropic and isotropic formulations. A further constitutive identification of foot skin is performed assuming an isotropic hyperelastic formulation, as proposed in Eqs (2), (3) and (4). The isotropic constitutive parameter is identified accounting for results from compression tests along the skin thickness (32), while the tensile behaviour is evaluated by data from tensile tests developed along the principal axis of the skin (26). The achieved constitutive parameters are reported in Table 2.

The developed constitutive formulations are implemented within ABAQUS 6.8 (Dassault Systèmes Simulia Corp., Providence, RI, USA) to specify the skin mechanical response within the finite element model of the foot. Numerical analyses of the ankle movements, as the dorsiflexion/plantarflexion, the inversion/eversion and the abduction/adduction, are performed accounting for both the anisotropic and the isotropic configurations of the skin.

Results

To highlight the anisotropic mechanical behaviour of the skin numerical analyses that interpret several movements of the foot are performed. In detail, abduction/adduction movements are analysed between +15° and −15° (38), eversion/inversion between +10° and −10° (37) while the movements of dorsiflexion and plantarflexion ranged between +20° and −20° (39–41).

Both isotropic and anisotropic formulations of skin are assumed to identify the influence of the collagen fibres distribution and to address the optimal configuration of skin tissue. With regard

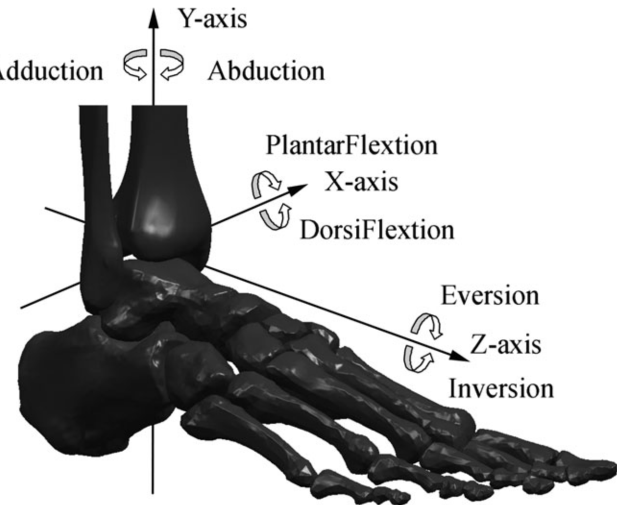

Fig. 4. Definition of the axis and of the movements of the ankle.

TABLE 2. Isotropic hyperelastic constitutive parameters adopted for skin mechanical characterization

K_v (MPa)	r	C_1 (MPa)	α_1
1.06×10^2	0.42×10^0	2.64×10^1	1.22×10^1

TABLE 1. Anisotropic hyperelastic constitutive parameters adopted for skin mechanical characterization

K_v (MPa)	r	C_1 (MPa)	α_1	C_4 (MPa)	α_4
3.9×10^1	1.40×10^0	9.55×10^{-1}	2.31×10^0	6.47×10^0	5.48×10^0

to the different ankle movements, the distribution of the maximum principal stress along specific cleavage lines is reported in Figs 5, 6 and 7, for 20° dorsiflexion, 15° abduction and 10° inversion movements respectively. The diagrams show the different mechanical response between isotropic (black lines) and anisotropic (grey lines) configurations. The anisotropic configuration of the skin entails lower stress values than the isotropic configuration. In detail, when the same cinematic condition of the foot is investigated, the maximum principal stress field is about 70% lower. With regard to the anisotropic configuration of the skin, in Fig. 8 the contour of the maximum principal stress is reported for the different ankle movements, as 20° dorsiflexion, 15° abduction and 10° inversion.

Discussion and conclusions

The investigation of the skin biomechanical response is faced with relevant problems because of the complex distribution of fibre reinforcing elements and the strongly non-linear mechanical behaviour. The numerical approach, integrated with experimental data, accounts for the actual mechanical behaviour of the tissues and the configuration of the biological structures. Hyperelastic models are used for representing

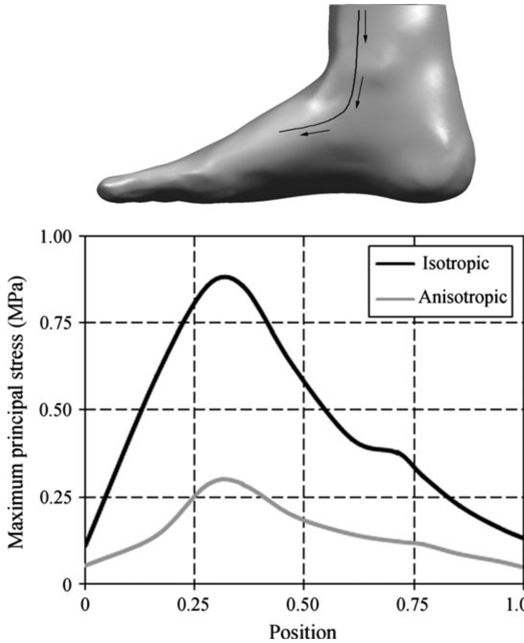

Fig. 6. Distribution of the maximum principal stress along a specific cleavage line (as depicted on the foot model) during the abduction movement. Results are reported for both isotropic (black line) and anisotropic (grey line) skin configurations.

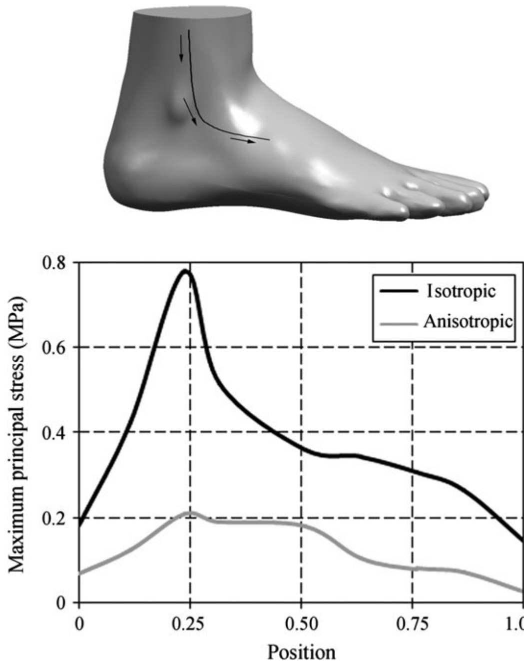

Fig. 7. Distribution of the maximum principal stress along a specific cleavage (as depicted on the foot model) line during the inversion movement. Results are reported for both isotropic (black line) and anisotropic (grey line) skin configurations.

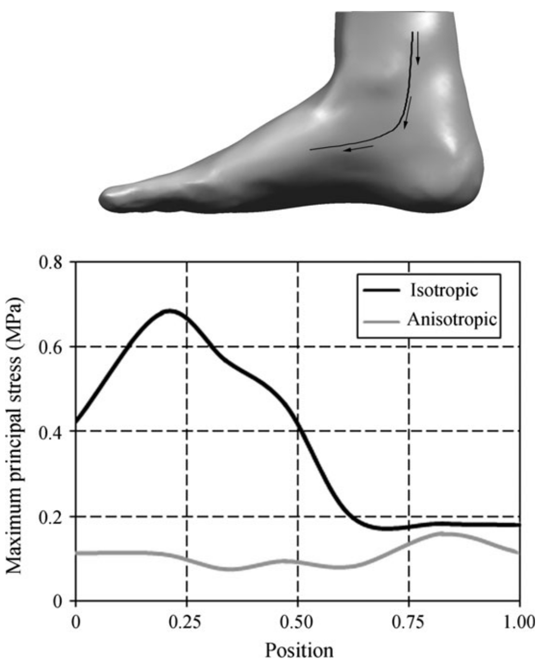

Fig. 5. Distribution of the maximum principal stress along a specific cleavage line (as depicted on the foot model) during the dorsiflexion movement. Results are reported for both isotropic (black line) and anisotropic (grey line) skin configurations.

soft tissues with regard to the material and geometric non linearity. The anisotropic characteristics induced by collagen fibres are considered by fibre-reinforced hyperelastic models.

More in detail, this work proposes a computational method for the definition of the

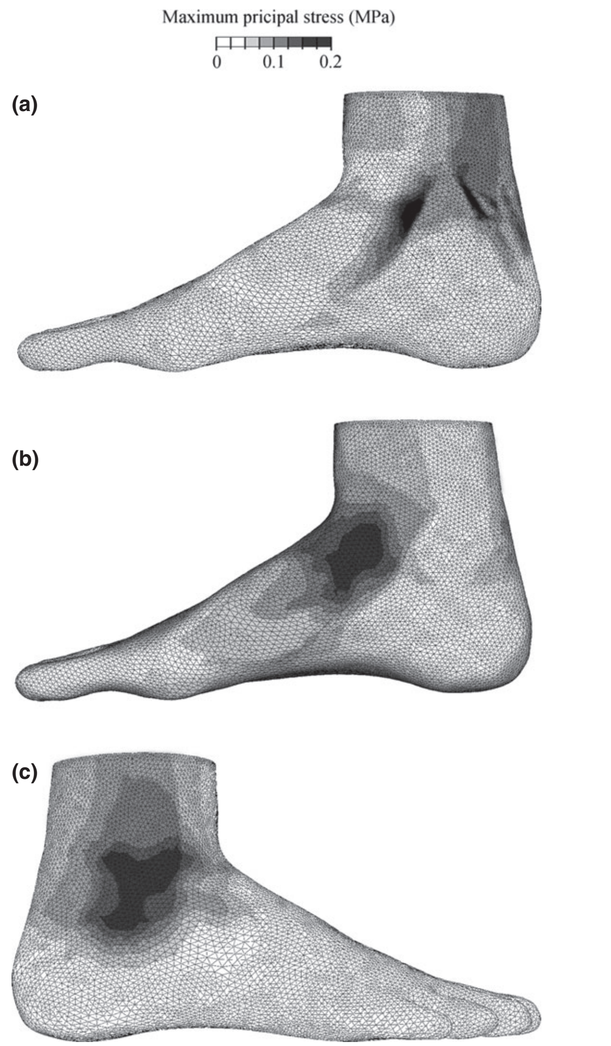

Fig. 8. Contour of maximum principal stress within the skin model during the 20° of dorsiflexion (a), 15° of abduction (b) and 10° of inversion (c) movements. Results are reported for the skin anisotropic configuration.

distribution of skin collagen fibres on the basis of experimental and histological data (3–5, 7, 9).

The numerical approach developed allows to describe the real mechanical behaviour of the skin with particular regard to the fibres contribution.

The numerical methods make it possible to evaluate the influence of the specific configuration of the skin on the structural behaviour of the foot. Different numerical analyses are performed accounting for isotropic and anisotropic skin configurations. With regard to the same foot movement, lower stress values are achieved when the anisotropic formulation is assumed, suggesting the optimal distribution of collagen fibres within the skin.

More refined constitutive formulations should be developed to characterize the skin mechanical behaviour to account for dissipative phenomena, as viscous and damage ones. Such analysis should provide a more comprehensive evaluation of the tissues functionality, with particular regard to degenerative situations. Nevertheless, complex constitutive formulations, as visco-hyperelastic and visco-hyperelasto-damage models (42), have been already provided for soft biological tissues, more experimental investigations are required for the reliable application to foot skin.

The here proposed numerical model of the skin must be integrated with further activities developed on other biological structures of the foot (34, 35, 43). The aim was the definition of a numerical model of the overall foot. Such model will make it possible to investigate the mechanical response of the different biological tissues and to evaluate, for example, the interaction phenomena occurring between foot and footwear products.

References

1. Minns RJ, Soden PD, Jackson DS. The role of the fibrous components and ground substance in the mechanical properties of biological tissues: a preliminary investigation. J Biomech 1973; 6: 153–165.
2. Reihsner R, Menzel EJ. On the orthogonal anisotropy of human skin as a function of anatomical region. Connect Tissue Res 1996; 34: 145–160.
3. Langer K. On the anatomy and physiology of the skin, I. The cleavability of the cutis. Br J Plast Surg 1978; 31: 3–8.
4. Langer K. On the anatomy and physiology of the skin, II. Skin tension by Professor K. Langer, presented at the meeting of 27th November 1861. Br J Plast Surg 1978; 31: 93–106.
5. Cox CJ. The cleavage lines of the skin. Br J Surg 1941–1942; 29:234–240.
6. Bulacio Nunez AW A new theory regarding the lines of skin tension. Plast Reconstr Surg 1974; 53: 663–669.
7. Borges AF. Relaxed skin tension lines (RSTL) versus other skin lines. Plast Reconstr Surg 1984; 73: 144–150.
8. Iberall AS. The use of lines of non extension to improve mobility in full pressure suits, AMRL-TR-64-118. Wright-Patterson AFB, OH: Rand Development Corporation report to Behavioral Sciences Laboratory, 1964.
9. Marreiros SSP. Skin strain field analysis of the ankle joint. Master's Thesis, Instituto Superior Técnico, Universidade Tecnica de Lisboa, 2010.
10. Andermahr J, Jubel A, Elsner A, Schulz-Algie PR, Schiffer G, Koebke

J. Die Hautspaltlinnien und die schnittführung bei Fuβoperationen. Orthopäde 2007; 36: 265–272.
11. Cheung JT-M, Zhang M. A 3-dimensional finite element model of the human foot and ankle for insole design. Arch Phys Med Rehabil 2005; 86: 353–358.
12. Cheung JT-M, Nigg BM. Clinical applications of computational simulation of foot and ankle. Sport Ortho Traumatol 2007; 23: 264–271.
13. Yu J, Cheung JTM, Fan Y, Zhang Y, Leung AKL, Zhang M. Development of a finite element model of female foot for high heeled shoe design. Clin Biomech 2008; 23: S31–S38.
14. Wang KTD, Wang C, Wang X, Liu A, Nester CJ, Howard D. An in vivo experimental validation of a computational model of human foot. J Bionic Eng 2009; 2009: 387–397.
15. Natali AN, Forestiero A, Carniel EL, Pavan PG, Dal Zovo C. Investigation of foot plantar pressure: experimental and numerical analysis. Med Biol Eng Comput 2010; 48: 1167–1174.
16. Gu YD, Li J, Ren X, Lake MJ, Zeng Y. Heel skin stiffness effect on the hind foot biomechanics during heel strike. Skin Res Technol 2010; 16: 291–296.
17. Sopher R, Nixon J, McGinnis E, Gefen A. The influence of foot posture, support stiffness, heel pad loading and tissue mechanical properties on biomechanical factors associated with a risk of heel ulceration. J Mech Behav Biomed 2011; 4: 572–582.
18. Lee Y, Hwang K. Skin thckness of Korean adults. Surg Radiol Anat 2002; 24: 183–189.
19. Overgaard Olsen L, Takiwaki H, Serup J. High-frequency ultrasound characterization of normal skin. Skin thickness and echographic density of 22 anatomical sites. Skin Res Technol 1995; 1: 74–80.
20. Thoolen M, Ryan TJ, Bristow I. A study of the skin of the sole of the foot using high-frequency ultrasonography and histology. The Foot 2000; 10: 14–17.
21. Natali AN, Carniel EL, Pavan PG. Modelling of mandible bone properties in the numerical analysis of oral implant biomechanics. Comput Methods Programs Biomed 2010; 100: 158–165.
22. Forestiero A, Carniel EL, Natali AN. Biomechanical behaviour of ankle ligaments: constitutive formulation and numerical modelling. Comput Methods Biomech Biomed Eng 2014; 17: 395–404.
23. Natali AN, Fontanella CG, Carniel EL. Constitutive formulation and numerical analysis of the heel pad region. Compt Methods Biomech Biomed Eng 2012; 15: 401–409.
24. Brown CP, Nguyen TC, Moody HR, et al. Assessment of common hyperelastic constitutive equations for describing normal and osteoarthritic articular catilage. Proc Inst Mech Eng H 2009; 223: 643–652.
25. Goske S, Erdemir A, Petre M, Budhabhatti S, Cavanagh PR. Reduction of plantar heel pressures: insole design using finite element analysis. J Biomech 2006; 39: 2363–2370.
26. Ankersen J, Birkbeck AE, Thomson RD, Vanezis P. Puncture resistance and tensile strength of skin simulants. Proc Instn Mech Eng Part H 1999; 213: 493–501.
27. Kvistedal YA, Nielsen PM. Estimating material parameters of human skin in vivo. Biomech Model Mechanobiol 2009; 8: 1–8.
28. Ruvolo EC, Stamatas GN, Kollias N. Skin Viscoelasticity displays site and age dependent angular anisotropy. Skin Pharmacol Physiol 2009; 20: 313–321.
29. Lokshin O, Lanir Y. Viscoelasticity and preconditioning of rat skin under uniaxial stretch: microsrtuctural constitutive characterization. ASME J Biomech Eng 2009; 131: 0331009.
30. Jor JWY, Nash MP, Nielsen PMF, Hunter PJ. Modelling the mechanical properties of human skin: towars a 3D discrete fibre model. Eng Med Biol Soc, 2007;6640–6643. EMBS 2007. 29th Annual International Conference of the IEEE.
31. Natali AN, Carniel EL, Gregersen H. Biomechanical behaviour of oesophageal tissues: material and structural configuration, experimental data and constitutive analysis. Med Eng Phy 2009; 31: 1056–1062.
32. Shergold OA, Fleck NA, Radford D. The uniaxial stress versus strain response of pig skin and silicone rubber at low and high strain rates. Int J Impact Eng 2006; 32: 1384–1402.
33. Natali AN, Forestiero A, Carniel EL. Parameters identification in constitutive models for soft tissue mechanics. Russian J Biomech 2009; 13: 29–39.
34. Fontanella CG, Forestiero A, Carniel EL, Natali AN. Analysis of heel pad tissues mechanics at the heel strike in bare and shod conditions. Med Eng Phys 2013; 35: 441–447.
35. Fontanella CG, Matteoli S, Carniel EL, Wilhjel JE, Virga A, Corvi A, Natali AN. Investigation on the load-displacement curves of a human healthy heel pad: in vivo compression data compared to numerical results. Med Eng Phy 2012; 34: 1253–1259.
36. Natali AN, Fontanella CG, Carniel EL, Miller-Young JE. Biomechanical behaviour of heel pad tissue. Experimental testing, constitutive formulation, and numerical modelling. J Eng Med 2011; 225: 449–459.
37. Siegler S, Udupa JK, Ringleb SI, Imhauser CW, Hirsch BE, Odhner D, Saha PK, Okereke E, Roach N. Mechanics of the ankle and subtalar joints revealed through a 3D quasi-static stress MRI technique. J Biomech 2005; 38: 567–578.
38. Lapointe SJ, Siegler S, Hillstrom H, Nobilini RR, Mlodzienski A, Techner L. Changes in the flexibility characteristics of the ankle complex due to damage to the lateral collateral ligaments: an in vitro and in vivo study. J Orthop Res 1997; 15: 331–341.
39. Allinger TL, Engsberg JR. A method to determine the range of motion of the ankle joint complex, in vivo. J Biomech 1993; 26: 69–76.
40. Fong CM, Blackburn JT, Norcross MF, McGrath M, Padua DA. Ankle-dorsiflexion range of motion and landing biomechanics. J Athl Train 2011; 46: 5–10.
41. Nordin M, Frankel VH. Basic biomechanics of the musculoskeletal system, 2nd edn. Philadelphia, PA: Lea & Febiger, 1989: xxiii, 323pp.
42. Natali AN, Carniel EL, Pavan PG, Sander FG, Dorow C, Geiger M. A visco-hyperelastic-damage constitutive model for the analysis of the biomechanical response of the periodontal ligament. ASME J Biomech Eng 2008; 130: 031004.
43. Pavan PG, Stecco C, Darwish S, Natali AN, De Caro R. Investigation of the mechanical properties of the plantar aponeurosis. Surg Radiol Anat 2011; 33: 905–911.

Address:
C. G. Fontanella
Centre of Mechanics of Biological Materials
University of Padova
Via F. Marzolo, 9
I-35131, Padova
Italy
Tel: +39 (0)49 827 5605
Fax: +39 (0)49 827 5604
e-mail: chiaragiulia.fontanella@unipd.it